Reactivity between Biphenyl and Precursor of Solvated Electrons in Tetrahydrofuran Measured by Picosecond Pulse Radiolysis in Near-Ultraviolet, Visible, and Infrared

Akinori Saeki,* Takahiro Kozawa, Yuko Ohnishi, and Seiichi Tagawa*

The Institute of Scientific and Industrial Research, Osaka University, 8-1 Mihogaoka, Ibaraki, Osaka 567-0047, Japan

Received: November 13, 2006; In Final Form: December 13, 2006

The initial decrease of solvated electrons in tetrahydrofuran (THF) upon addition of biphenyl was investigated by picosecond pulse radiolysis. Transient absorption spectra derived from the biphenyl radical anion (centered at 408 and 655 nm) and solvated electrons of THF (infrared) were successfully measured in the wavelength region from 400 to 900 nm by the extension of a femtosecond continuum probe light to near-ultraviolet using a second harmonic generation of Ti:sapphire laser and a CaF_2 plate. From the analysis of kinetic traces at 1300 nm considering the overlap of primary solvated electrons and partial biphenyl radical anion, C_{37}, which is defined by the solute concentration to reduce the initial yield of solvated electrons to $1/e$, was found to be 87 ± 3 mM. The rate constant of solvated electrons with biphenyl was determined as $5.8 \pm 0.3 \times 10^{10}$ M^{-1} s^{-1}. We demonstrate that the kinetic traces at both 408 nm mainly due to biphenyl radical anion and 1300 nm mainly due to solvated electrons are reproduced with high accuracy and consistency by a simple kinetic analysis. Much higher concentrations of biphenyl (up to 2 M) were examined, showing further increase of the initial yield of biphenyl radical anion accompanying a fast decay component. This observation is discussed in terms of geminate ion recombination, scavenging, delayed geminate ion recombination, and direct ionization of biphenyl at high concentration.

1. Introduction

Radiation-initiated reactions and the reactivity of the generated intermediates[1] have attracted much attention in not only the basic science of radiation chemistry but also in associated fields such as biochemistry, radiotherapy, environmental chemistry, and lithography. Solvated (or hydrated) electrons in, e.g., water,[2−19] alcohols,[20−24] ethers,[25−37] amines,[25,38,39] and ionic liquids,[40,41] have been a major class of transient species and subjected to intensive theoretical and experimental investigations in terms of structures, reactivity, radiation-induced yield, etc. Since the discovery of hydrated electrons in water by Hart et al.,[2] these kinds of short-lived species have occupied an important place in radiation chemistry. Hunt and co-workers[3−5] focused on the decrease of the initial yield of hydrated electrons in water upon addition of various kinds of solutes, and demonstrated that the fraction of decrease f was expressed by an exponential as a function of solute concentration:

$$f = \exp(-[S]/C_{37}) \quad (1)$$

where $[S]$ is the concentration of the scavenger and C_{37} is a constant which depends on solvent and solute. C_{37} can be understood as the solute concentration which reduces the initial yield of solvated electrons to $1/e$ (37%). Acetone and positive or negative ions have been employed as the scavenger of hydrated electrons in water. The mechanism of the initial decrease has been discussed from the viewpoints such as (i) reaction with precursor of hydrated electrons,[4−8] (ii) time-dependent rate constant,[42−44] (iii) direct formation of encounter pairs at high concentration,[45] and (iv) tunneling model as was observed in organic glasses[46] or donor−acceptor system.[47] The detailed investigations have settled this issue, resulting in that "(i) reaction with precursor" is the most probable.

To the best of our knowledge, although numerous researches on C_{37} have been performed for water and alcohols, C_{37} of tetrahydrofuran (THF), which is one of the typical ethers and has been utilized as a good solvent for many aromatics and polymers, has not been well surveyed, in particular on the picosecond time scale. Recently our group, collaborating with Brookhaven National Laboratory, investigated the reactivity of solvated electrons in THF (e_{sol}^-) with several kinds of ionic and nonionic photo acid generators (PAGs)[37] in the concentration range of $20 \sim 200$ μM by means of nanosecond pulse radiolysis, showing that reaction rates of ionic PAGs are higher than those of nonionic PAGs. In order to shed light on the nature of reaction mechanism between e_{sol}^- and the PAGs and other polymeric materials, it is important to gain more information on the reactivity of e_{sol}^-.

In this paper, we adopted biphenyl (BP) as the scavenger of e_{sol}^- and of its precursor, because BP has been widely used in radiation chemistry and its radical anion ($BP^{\bullet -}$) has strong photo absorption at around 408 and 655 nm, of which extinction coefficients are 40 000 and 12 500 M^{-1} cm^{-1}, respectively.[34,35,48,49] For a comprehensive study on the reactivity of e_{sol}^-, it is of significant help to measure and analyze the formation of $BP^{\bullet -}$ at 408 and 655 nm and decay of e_{sol}^- at infrared (IR). While the absorption maximum of e_{sol}^- is reported to be at 2.1 μm,[25,26,34,35] its broad absorption is stretched to visible region. Because of a technical reason, 1300 nm was taken as the probe wavelength for the decay of e_{sol}^-. Although $BP^{\bullet -}$ has a relatively strong absorption at 655 nm which can be covered by our picosecond pulse radiolysis system[50] with high signal-to-noise (S/N) ratio, strong contribution from e_{sol}^- still remains at this

* Corresponding authors. E-mails: saeki-a@sanken.osaka-u.ac.jp(A.S.), tagawa@sanken.osaka-u.ac.jp(S.T.). Tel: +81-6-6879-8502. Fax: +81-6-6876-3287.

10.1021/jp067520m CCC: $37.00
Published on Web 01/27/2007

wavelength. Therefore, using a near-ultraviolet-enhanced laser pulse,[51] we extended the white light continuum to the near-ultraviolet (UV) where the strongest absorption of $BP^{\bullet-}$ exists and the contribution from e_{sol}^- is minimized. We demonstrate for the first time a picosecond pulse radiolysis of e_{sol}^- and $BP^{\bullet-}$ in the wavelength regions of a continuous near-UV−visible−near-IR (400−900 nm) and a discrete IR (1300 nm), for the comprehensive study on the reactivity of BP with the precursor of e_{sol}^- within time resolution and with e_{sol}^- in picosecond time scale under diffusion control.

2. Experimental

An electron beam as an irradiation source was provided by 27 MeV L-band linear accelerator (linac) at the Institute of Scientific and Industrial Research (ISIR), Osaka University with a pulse duration of ∼15 ps (full-width at half-maximum, FWHM), which is not magnetically compressed in the present study. A femtosecond laser pulse amplified in a regenerative amplifier (wavelength 800 nm, energy 0.7 mJ/pulse, pulse duration < 130 fs, repetition rate 960 Hz) was provided by a femtosecond Ti:sapphire laser system (Spectra Physics Inc.). The laser and linac were synchronized via common radio frequency of around 81 MHz. The details of the synchronization between the laser system and the linac, and timing/trigger system were reported previously.[52]

For transient spectroscopy in near-UV region, the amplified laser was passed through a 1 mm-thick KDP crystal, converting to a second harmonic generation (SHG, 400 nm). The SHG was then focused into a 3 mm thick CaF_2 plate, yielding a wavelength-extended continuum from ca. 380 to 600 nm (wavelength region near the edges is not applicable for a practical experiment because of the low stability and low intensity). The detail of this near-UV-enhanced continuum will be reported elsewhere.[51] The generation of white light in visible region was performed using a sapphire plate instead of a CaF_2 plate and a fundamental oscillation of Ti:sapphire laser (800 nm), following a scheme of the previous report.[50] The diverged continuum was parallelized by a $f = 50$ mm lens and transported from a laser room to the beam port which is shielded by 3 m wide concrete for prevention of radiation leak. The distance of the laser transport is about 10 m. The time difference between the electron beam and continuum was changed by an optical delay located before a sample. The electron beam and the continuum were coaxially introduced into a sample in a quartz cell. After passing through a sample, white light was transported to a monochromator (SP-2358, Princeton Instruments), separated into a spectrum component, and detected by a thermoelectrically cooled CCD camera (PIXIS400BR, Princeton Instruments) which has 400 × 1340 CCD elements and a 16-bit dynamic AD converter.

In the spectroscopy in IR region, a signal from an optical parametric amplifier (OPA, Spectra Physics Inc.) and an InGaAs detector were used. For the transient spectroscopy at 400 nm, the SHG light without converting to near-UV continuum was used to improve S/N ratio at this wavelength.

Infinity-pure grade tetrahydrofuran was purchased from Wako Corporation and used as received. Biphenyl was purchased from Tokyo chemical industry corporation and recrystallized in benzene. Samples were loaded in a quartz cell of which optical path is 2 cm and bubbled by Ar gas for at lease 5 min. All experiments were carried out at room temperature.

3. Results and Discussion

Transient photo absorption spectra in pure THF and THF solution of BP (20 and 100 mM) at 200 ps after the end-of-pulse are shown in Figure 1. The primary radiation-chemical reactions in THF containing BP are summarized below:[29]

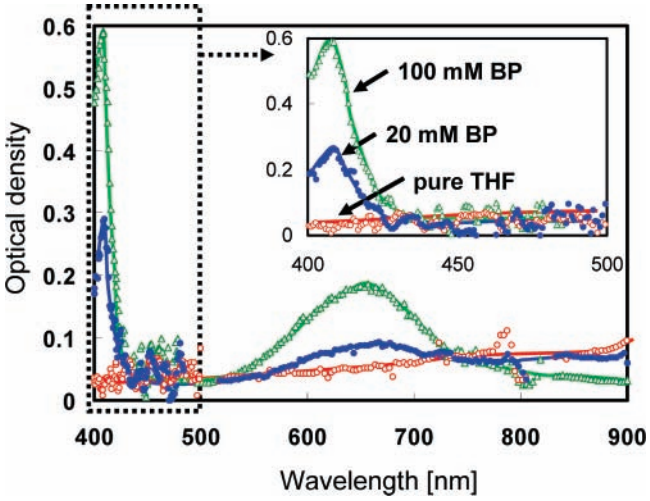

Figure 1. Transient photo absorption spectra in pure THF (open red circles, red line), THF solution of 20 mM biphenyl (closed blue circles, blue line), and THF solution of 100 mM biphenyl (open green triangles, green line) at 200 ps after the end-of-pulse. Each dot in near-UV region (ca. from 400 to 500 nm) and visible-near-IR region (ca. from 500 to 900 nm) was measured by averaging over 10 and 2 beam-probe shots, respectively.

$$\mathrm{THF} \rightsquigarrow \mathrm{THF}^{\bullet+} + e_{pre}^- \quad (2)$$

$$e_{pre}^- + n\mathrm{THF} \rightarrow e_{sol}^- \quad (3)$$

$$\mathrm{THF}^{\bullet+} + \mathrm{THF} \rightarrow \mathrm{THF}(-\mathrm{H})^{\bullet} + \mathrm{THF}(+\mathrm{H})^+ \quad (4)$$

$$e_{pre}^- + \mathrm{BP} \rightarrow \mathrm{BP}^{\bullet-} \quad (5)$$

$$e_{sol}^- + \mathrm{BP} \rightarrow \mathrm{BP}^{\bullet-} \quad (6)$$

$$e_{pre}^- + \mathrm{THF}(+\mathrm{H})^+ \rightarrow \text{products} \quad (7)$$

$$e_{sol}^- + \mathrm{THF}(+\mathrm{H})^+ \rightarrow \text{products} \quad (8)$$

$$\mathrm{BP}^{\bullet-} + \mathrm{THF}(+\mathrm{H})^+ \rightarrow \text{products} \quad (9)$$

A small portion of e_{sol}^- is lost by the reaction with radical species.

$$e_{sol}^- + \mathrm{THF}(-\mathrm{H})^{\bullet} \rightarrow \mathrm{THF}(-\mathrm{H})^- \quad (10)$$

In THF solution of BP, the formation of $BP^{\bullet-}$ is expressed by reactions 5 and 6. In Figure 1, the strong absorption peaks ascribed to $BP^{\bullet-}$ was clearly observed at ca. 408 and 655 nm which are identical to the spectrum measured by γ-radiolysis in a low-temperature matrix of methyl−THF,[49] while a broad absorption of e_{sol}^- in pure THF is seen from UV to IR. One would find that the contributions of e_{sol}^- at 408 nm and that of $BP^{\bullet-}$ at IR (1300 nm) are minimized. Since the absorption of $BP^{\bullet-}$ is strong, the absorbed dose for these experiments were reduced to ca. 33 ± 3 Gy which was estimated from the absorption of hydrated electrons in water with G value of 4.0−4.1 molecules $(100\ \mathrm{eV})^{-1}$.[14,17,53,54] We also calculated the absorbed dose from the absorption of $BP^{\bullet-}$ at 408 nm using G value of solvated electron in THF [2.7×10^{-7} mol J^{-1} at the end-of-pulse, equivalent to 2.6 molecules $(100\ \mathrm{eV})^{-1}$],[36] the extinction coefficient of $BP^{\bullet-}$ ($4 \times 10^4\ \mathrm{M}^{-1}\ \mathrm{cm}^{-1}$),[34,35,48,49] optical density of ∼0.6 with the optical length of 2 cm, and density of THF ($0.8833\ \mathrm{g\ cm}^{-3}$),[55] resulting in 32 ± 3 Gy which

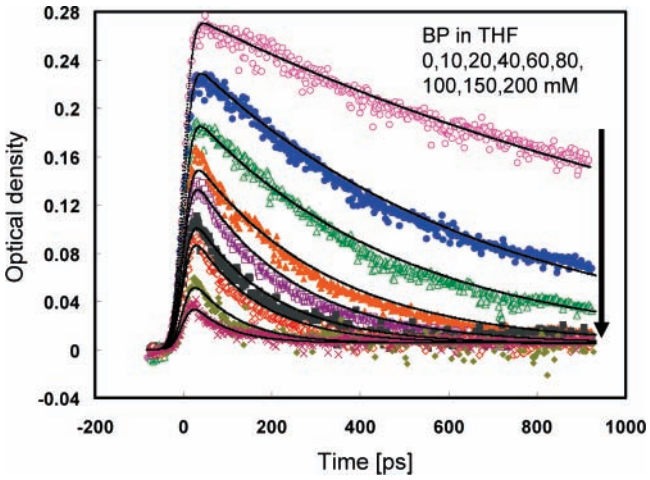

Figure 2. Kinetic traces at 1300 nm in THF solution of biphenyl, of which concentration are varied, 0 (open pink circles), 10 (closed blue circles), 20 (open green triangles), 40 (closed orange triangles), 60 (open purple squares), 100 (closed ocher squares), 100 (open red diamonds), 150 (closed yellow-green diamonds), and 200 mM (crosses). Each dot was measured by averaging over 2 beam-probe shots.

is consistent with that estimated from dosimetry by hydrated electrons in water. Note that the optical density of ~0.6 is based on the kinetic analysis (discussed later) of highly concentrated BP in THF at 408 nm after 500 ps when most of the e_{sol}^- is scavenged by BP. Therefore, a certain small fraction due to the recombination decays of e_{pre}^- and e_{sol}^- expressed by reactions 7 and 8 led to an underestimation of the absorbed dose.

Figure 2 shows the kinetic traces of e_{sol}^- monitored at 1300 nm in THF solution containing 0−200 mM BP. The solid lines in Figure 2 are the curves reproduced by kinetic analysis discussed later. With the increase of BP concentration, the decrease in the initial yield of e_{sol}^- was clearly observed. The decay rate was also accelerated with the BP concentration; however, at high concentration more than ca. 100 mM, the decay rate began to be milder, accompanied by a long life time component surviving to >500 ps. Although the absorption of $BP^{\bullet-}$ was reported to lie in only visible domain,[34,35,48,49] the tail extends into the IR region, which is pronounced in the presence of high concentration of BP. Regarding the pure THF, the decay is almost identical to the previous report monitored at 790 nm.[36]

In Figure 3a, the decrease in the fraction of initial yield of e_{sol}^- is plotted as a function of BP concentration. The fraction data depicted as open circles were obtained from the optical densities at the pulse end for each BP concentration normalized to that of pure THF. The contribution from the long-lived component at high concentration was subtracted depending on the BP concentration (this component is discussed later), although the effect of this subtraction is small, in particular, in low concentration regime. The fraction data were analyzed by a least-mean-square fitting of eq 1 (solid line), giving $C_{37} = 87 \pm 3$ mM. The closed circles and dotted line correspond to the increase of initial yield of $BP^{\bullet-}$ at 408 nm (discussed later). As was mentioned in the introduction, the mechanism of decrease in initial yield of solvated/hydrated electrons has been discussed[4−8] in terms of (i) reaction with precursor of solvated/hydrated electrons, (ii) time-dependent rate constant, (iii) direct formation of encounter pairs at high concentration, and (iv) tunneling model. Item ii has been analyzed in detail on the basis of Smoluchowski theory and diffusion constant derived from a rate constant, proving that this effect is much smaller than the experimental indication.[4,6] The effect of item iii was ruled out

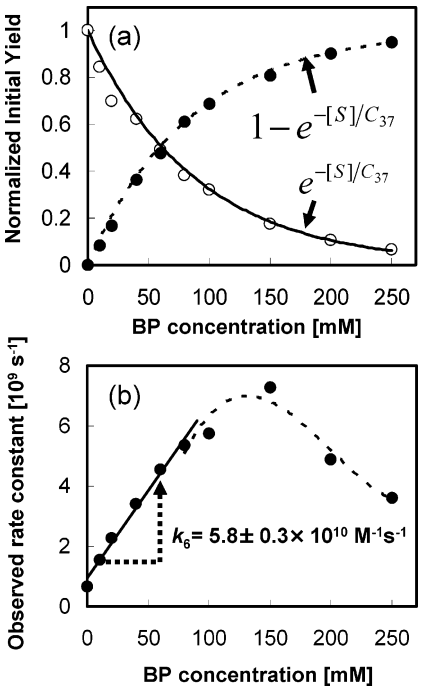

Figure 3. (a) Fraction of initial yield of e_{sol}^- based on the 1300 nm (open circles, solid line) and that of biphenyl radical anion based on 408 nm (closed circles, dotted line). Typical error in *y*-direction is ca. 0.06. (b) Observed rate constants as a function of biphenyl concentration obtained from 1300 nm kinetic traces.

from the main factor as well, because the contribution was found to be small. We should mention that an adjacent effect analogous to item iii can explain well the decrease of initial yield of radical cation in the presence of high concentration scavenger,[56] with additional consideration of an excluded volume effect and concentration-dependent reaction volume modifying Czapski's model.[45] The difference of reactivity between radical cation and electron with scavengers is that the former does not travel a long distance (except for high mobility hole[57−59]) before the diffusion of radical cation molecule starts, because it basically belongs to an ionized molecule. On the other hand, the electron ejected from a molecule via ionization travels for a certain distance to be thermalized before the solvation and subsequent diffusion. If a solute has a high reactivity with the non-thermalized electrons and/or precursor of solvated electron before the solvation completes, the initial yield of solvated/hydrated electrons is reduced.[60] As to the effect of item iv, it was also ruled out[4] by investigating the dependence of solutes and solvents, the reaction radii, the rate constants, and depth of potential.

Figure 3b shows the observed rate constant in the presence of BP monitored at 1300 nm. Since there are some contributions of $BP^{\bullet-}$ to the 1300 nm kinetics (confirmed later), the time range for the fitting analysis by exponential functions was shortened, e.g., 500 ps for 10 mM and 200 ps for 250 mM, so that the contribution of $BP^{\bullet-}$ formation followed by scavenging of e_{sol}^- was eliminated as much as possible. A good linearity was found at less than 80 mM, giving rate constant of reaction 6: $k_6 = 5.8 \pm 0.3 \times 10^{10}$ M^{-1} s^{-1}, while the observed rate constant began to be lower than the linear line and then fall at >200 mM. The bend of the curve is ascribed to the fact that the overlap of $BP^{\bullet-}$ formed by scavenging reaction under the diffusion process (reaction 6) becomes large in the high concentration region. For instance, the contribution of the $BP^{\bullet-}$ at 80 mM at 200 ps delay is ca. 10%, while that at 150 mM becomes comparable with that of e_{sol}^-. The overlap of $BP^{\bullet-}$

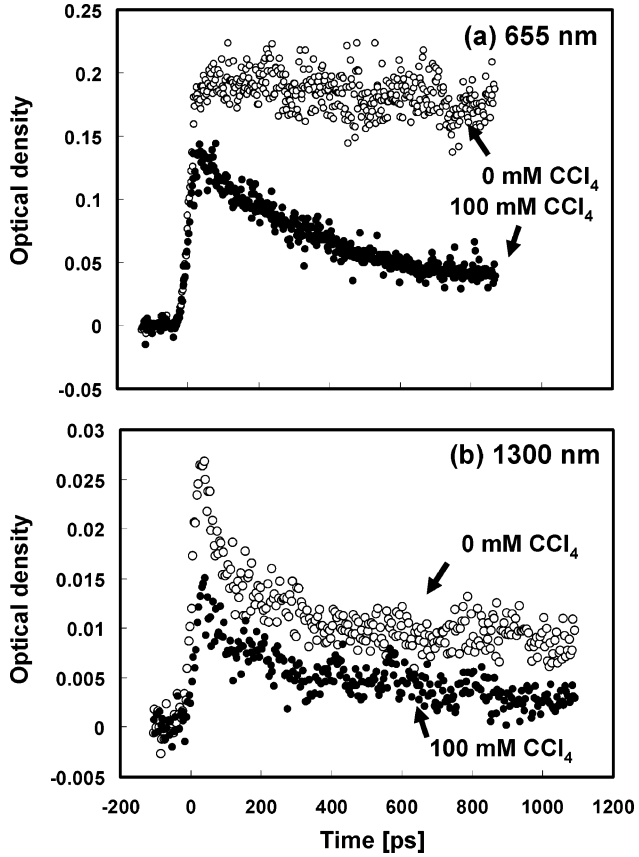

Figure 4. Kinetic traces in THF solution of 250 mM biphenyl with (closed circles) and without (open circles) 100 mM CCl_4 monitored at (a) 655 and (b) 1300 nm. Each dot was measured by averaging over 2 beam-probe shots.

and e_{sol}^- at 1300 nm was examined by addition of carbontetrachloride (CCl_4). Panels a and b of Figure 4 show the kinetic traces in THF solution of 250 mM BP with and without 100 mM CCl_4 monitored at 655 and 1300 nm, respectively. The additional scavenging reactions by CCl_4 are summarized below:

$$e_{pre}^- + CCl_4 \rightarrow CCl_3^{\bullet} + Cl^- \quad (11)$$

$$e_{sol}^- + CCl_4 \rightarrow CCl_3^{\bullet} + Cl^- \quad (12)$$

$$BP^{\bullet -} + CCl_4 \rightarrow CCl_3^{\bullet} + Cl^- + BP \quad (13)$$

It is apparently seen that the $BP^{\bullet -}$ at 655 nm were scavenged by CCl_4 (reaction 13). Regarding the kinetics at 1300 nm, the initial yield of e_{sol}^- was decreased further upon addition of CCl_4, due to reactions 11 and 12. The initial spike-like decay of e_{sol}^- within less than ca. 150 ps was not clearly observed because of the lack in enough time resolution and low S/N ratio; however, the decay in the long time region (>ca. 400 ps) was found to be accelerated by the scavenging effect (reaction 13), suggesting the existence of $BP^{\bullet -}$ contribution to the long lifetime component at 1300 nm.

The k_6 obtained here is close to the value of $3.9 \pm 0.1 \times 10^{10}$ M^{-1} s^{-1}, which was measured by Renou and Mostafavi et al.[34,35] using nanosecond pulse radiolysis at 1000 nm. As mentioned in the introduction, we also reported that the lower value of rate constant between nonionic PAG and e_{sol}^- was $6 \pm 1 \times 10^{10}$ M^{-1} s^{-1},[37] which was also measured by nanosecond pulse radiolysis at 900 nm. The other nonionic PAG indicated higher value of around $1.0 \pm 0.1 \times 10^{11}$ M^{-1} s^{-1}; however, the volumes of these PAGs are much larger than BP, and thus, the larger reaction radii would account for the large rate constant. These rate constants are, however, roughly a factor of 2−3 lower than the first report ($k_6 = 1.1 \pm 0.3 \times 10^{11}$ M^{-1} s^{-1})[26] of BP and e_{sol}^-. Renou and Mostafavi et al.[34] pointed out that this value was derived from the analysis of $BP^{\bullet -}$ formation at 630 nm where a large contribution of e_{sol}^- exists, leading to the overestimation of rate constant. On the contrary, ionic PAGs[37] gave the large k values reaching $1.9 \pm 0.1 \times 10^{11}$ M^{-1} s^{-1}. This might be explained, in addition to the large reaction radii, by the dissociation of ionic PAGs in THF, analogous to the large rate constant between hydrated electrons in water and ionic species like sodium ion.[4] The diffusion-controlled rate constant (k_{diff}) in THF based on macroscopic viscosity is given by $k_{diff} = 8RT/3\eta \approx 1.4 \times 10^{10}$ M^{-1} s^{-1}.[37] This value is from 4 to 5 times smaller than the observed rate constant (k_6). This discrepancy would be linked to that the microscopic viscosity is significantly lower than macroviscosity as asserted by Wishart et al.[40] The limit of diffusion-controlled rate constant estimated from pulse radiolysis experiments was reported to be 1.7×10^{11} M^{-1} s^{-1} by Kadhum and Salmon,[30] which is still a little smaller than the k observed for ionic PAGs.[37]

Hunt and co-workers[4] predicted that the C_{37} could be correlated with high concentration rate constant k between hydrated (solvated) electron and solute, i.e., $k \cdot C_{37}$ = constant (s^{-1}) which is specific to the solvent. They also insisted that the C_{37} is not dependent on solvation time and static dielectric constant.[5] For hydrated electron in water, solvated electron in ethanol, and that in ethylene glycol, they deduced $k \cdot C_{37} = 1.0 \pm 0.2 \times 10^{10}$, $1.3 \pm 0.3 \times 10^9$, and 5×10^9 s^{-1}, respectively.[4] The $k \cdot C_{37}$ obtained here for BP in THF was $5.1 \pm 0.4 \times 10^9$ s^{-1}, which is close to that in ethylene glycol. The relationship $k \cdot C_{37}$ = constant is, however, not reliable, as pointed out by Jonah et al.[6] from the experiments of hydrated electron in water. While the k is obtained from the decay of solvated electrons during their and solute's diffusion process, the C_{37} reflects the reactivity of electrons with solute before thermalization, presolvation, and solvation of electrons. The diffusion of solute and solvated electron is much slower than the latter processes. If the time scales of these processes are simply proportional to the k, it would be correlated linearly with C_{37}; however, many factors such as the electron energy before thermalization, depth of localization site of solvated electron, and spectrum change are, in actual, involved in a complex manner, and thus, the $k \cdot C_{37}$ relationship is not supported to date as claimed by Jonah et al.[6] It is, however, no doubt that the C_{37} is dependent on solute and solvent. The C_{37} of BP in THF presented here is close to C_{37} of phenanthrene in ionic liquid (84 mM),[40] rather than BP in methanol (300 mM), ethanol (190 mM), and 1-propanol (180 mM).[4] Although the diffusion-controlled rate constant of THF (1.4×10^{10} M^{-1} s^{-1} mentioned in the previous paragraph) is 3 orders of magnitude higher than that of ionic liquid (1.5×10^7 M^{-1} s^{-1}),[40] no significant difference in C_{37} was found for these solvents, supporting the k is not correlated with C_{37}.

Using the observed rate constant $k_6 = 5.8 \pm 0.3 \times 10^{10}$ M^{-1} s^{-1} and $C_{37} = 87 \pm 3$ mM, we analyzed the kinetic traces at 1300 nm based on reactions 2−8. The ionization (reaction 2) and solvation (reaction 3) were regarded as a stepwise formation, because they are too fast for the time resolution of our system. Scavenging reaction of precursor of e_{sol}^- with BP expressed by reaction 5 was also assumed as a stepwise reaction, while the decrease of initial yield of e_{sol}^- was taken into consideration using C_{37}. Reaction 7, geminate ion recombination between e_{pre}^- and $THF^{\bullet +}$ was not included in the calculation, because it is too fast to be detected by the present experimental apparatus.

Reaction 8, geminate ion recombination between e_{sol}^- and $THF^{\bullet+}$ on picosecond time scale, has been analyzed previously by stretched exponential functions;[36] however, we adopted a common exponential function for simplicity, because there was no significant difference among these functions up to ca. 900 ps. Reaction 9, delayed geminate ion recombination between $BP^{\bullet-}$ and $THF^{\bullet+}$, was not incorporated, because no decay was observed for $BP^{\bullet-}$ at 408 nm even in the presence of high BP concentration up to 200 mM. This treatment is supported by the bulk recombination rate constant[34] k_9 of $3.7 \pm 0.2 \times 10^{11}$ M^{-1} s^{-1} and the low $BP^{\bullet-}$ concentration of 7.5 μM at maximum, giving a few hundreds of nanosecond for the life time. However, at much higher concentration of BP (e.g., 1 M), the contribution of reaction 9 begins to appear. The detail is discussed in the last part of this paper. Consequently, the fitting parameter is the ratio of extinction coefficient at 1300 nm between $BP^{\bullet-}$: $\epsilon_{BP}{}^{\bullet-}$(1300 nm) and e_{sol}^-:$\epsilon_{esol}{}^-$(1300 nm). The solid lines in Figure 2 convoluted using the previously reported protocol[61] was successfully reproduced using $\epsilon_{BP}{}^{\bullet-}$(1300 nm)/$\epsilon_{esol}{}^-$(1300 nm) $= 2 \times 10^{-2}$. On the basis of the G value of e_{sol}^-,[36] $\epsilon_{esol}{}^-$(1300 nm) and $\epsilon_{BP\cdot-}$(1300 nm) were estimated to be 1.8×10^4 and 3.5×10^2 M^{-1} cm^{-1}, respectively. The $\epsilon_{BP}{}^{\bullet-}$(1300 nm) is 2.8% of that at 655 nm, which is a reasonable value from the viewpoint of spectrum shape of $BP^{\bullet-}$[34,35,48,49] and e_{sol}^-,[25,26,34,35] supporting the reliability of the fitting results.

Figure 5a shows the kinetic traces at 408 nm in THF solution of BP. The solid lines are the fitting curves obtained by the same procedure abovementioned, using $\epsilon_{BP\cdot-}$(408 nm)/ϵ_{esol-}(408 nm) $=$ 15 as the ratio of the extinction coefficients. The ϵ_{esol-}(408 nm) was estimated to be 2.7×10^3 M^{-1} cm^{-1}, which is 27% compared to $\epsilon_{esol}{}^-$(1300 nm). This extinction coefficient is consistent with the literature,[25,26,34,35] and reasonable by the spectrum shape shown in Figure 1. The fitting parameters used are summarized in Table 1. Example of the fitting curve resolved by each component is shown in Figure 5b.

The increase of initial yield of $BP^{\bullet-}$ at 408 nm subsequent to the reaction between e_{pre}^- and BP is superimposed in Figure 3a as the closed circles, where the contribution of e_{sol}^- was subtracted from the data depending on the BP concentration. Note that the effect of this subtraction is quite small because of the high extinction coefficient of $BP^{\bullet-}$ at 408 nm as mentioned above. The dotted line represent the complementary of eq 1, namely, $1 - \exp(-[S]/C_{37})$. The curve is in good agreement with the plotted data, reinforcing the comprehensive studies about the scavenging reaction of e_{sol}^- and precursor of e_{sol}^- by BP.

At room temperature, the diffusion constant of BP molecule in THF ($D_{BPinTHF}$) is estimated to be 3.51×10^{-5} cm^2 s^{-1} from that in infinite dilution of 1-butanol ($D_{BPinBuOH} = 0.63 \times 10^{-5}$ cm^2 s^{-1}, viscocity $\eta = 2.544$ mPa s) and η of THF (0.456 mPa s).[62] The diffusion constant of biphenyl radical anion in THF ($D_{BP^{\bullet-}inTHF}$) was reported to be 2.4×10^{-5} cm^2 s^{-1}.[63] These values ($D_{BPinTHF}$ and $D_{BP^{\bullet-}inTHF}$) are less than 25% of the diffusion constant of solvated electrons in THF ($D_{esol}{}^- = 1.4 \times 10^{-4}$ cm^2 s^{-1}) reported previously,[64] and thus, the fluctuation in D_{BP} is not so effective for the following discussion. If one adopts the values of abovementioned $D_{esol}{}^-$ and $D_{BPinTHF}$, the reaction radius r between BP and e_{sol}^- is estimated to be 0.44 nm from the rate constant obtained in this study and the following relationship:

$$k = 4\pi r(D_{esol}{}^- + D_{BPinTHF}) \qquad (14)$$

This r is a reasonable value from the consideration of the size of biphenyl and solvated electron in THF,[31] supporting the results of the present study.

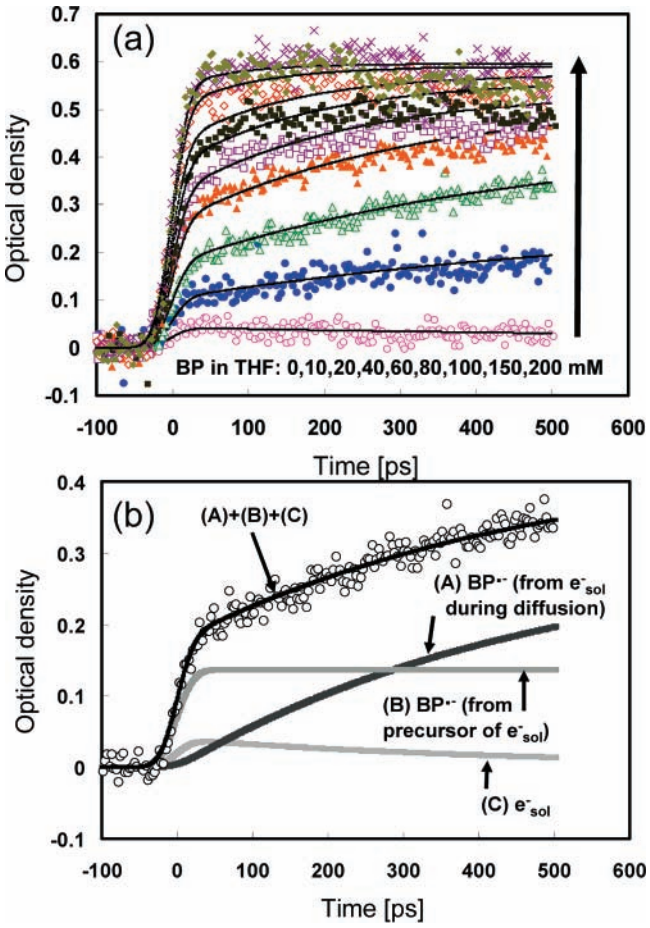

Figure 5. (a) Kinetic traces at 408 nm in THF solution of biphenyl, of which concentration are varied, 0 (open pink circles), 10 (closed blue circles), 20 (open green triangles), 40 (closed orange triangles), 60 (open purple squares), 100 (closed ocher squares), 100 (open red diamonds), 150 (closed yellow-green diamonds), and 200 mM (crosses). Each dot was measured by averaging over 10 beam-probe shots. (b) Kinetic traces at 408 nm in THF solution of 20 mM biphenyl (open circles). Each solid line represent the resolved component: (A) biphenyl radical anion formed by scavenging reaction of solvated electron in THF during diffusion process, (B) biphenyl radical anion formed by reaction with precursors of solvated electrons in THF within the time resolution, and (C) solvated electrons in THF which decay by charge recombination and scavenging reaction. Each dot was measured by averaging over 10 beam-probe shots.

TABLE 1: Parameters Used in the Fitting Analyses

parameter	value
k (e_{sol}^- + BP)[a]	5.8 ± 0.3 10^{10} M^{-1} s^{-1}
C_{37}	87 ± 3 mM
$\epsilon_{esol}{}^-$ at 1300 nm	1.8×10^4 M^{-1} cm^{-1}
$\epsilon_{BP}{}^{\bullet-}$ at 1300 nm	3.5×10^2 M^{-1} cm^{-1}
$\epsilon_{esol}{}^-$ at 408 nm	2.7×10^3 M^{-1} cm^{-1}
$\epsilon_{BP}{}^{\bullet-}$ at 408 nm	4.0×10^4 M^{-1} cm^{-1} [b]

[a] The e_{sol}^- and BP represent solvated electron in tetrahydrofuran and biphenyl, respectively. [b] Value from refs 34, 35, 48, and 49.

We measured the kinetic traces of $BP^{\bullet-}$ in the presence of much higher concentration of BP up to 2 M. The results monitored at 400 nm are shown in Figure 6. Above 1 M BP, the initial yield of $BP^{\bullet-}$ was increased further by about 10%, accompanying a fast decay component. This experimental fact would be explained in terms of the geminate ion recombination of e_{pre}^- with $THF(+H)^+$ (reaction 7), the scavenging reaction of e_{pre}^- by BP (reaction 5), and subsequent delayed geminate ion recombination of $BP^{\bullet-}$ with $THF(+H)^+$ (reaction 9). The observed G value of e_{sol}^- [2.6 molecules $(100\ eV)^{-1}$][36] is about

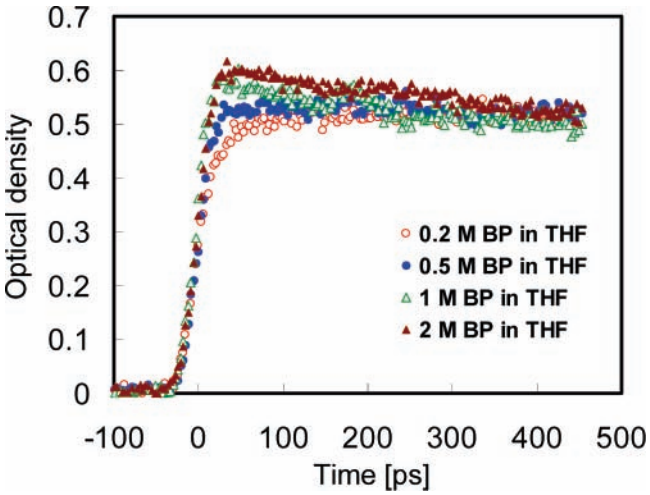

Figure 6. Kinetic traces at 400 nm in THF solutions of 0.2 (red open circles), 0.5 (blue closed circles), 1 (green open triangles), and 2 (brown closed triangles) M biphenyl. Each dot was measured by averaging over 2 beam-probe shots.

two-thirds compared to that of hydrated electron in water [4.0 ~ 4.1 molecules $(100\ eV)^{-1}$].[14,17,53,54] The small G value was explained by a fast decay within the time resolution,[36] which would be ascribed mainly to the geminate ion recombination of e_{pre}^- (reaction 7). By addition of highly concentrated Cd^{2+} or cystamine (ca. 5 M), Wolff and Hunt et al.[3c] reported that G value of product [4.8 molecules $(100\ eV)^{-1}$] was higher than that of hydrated electron in water [4.0 molecules $(100\ eV)^{-1}$], suggesting that the yield of electron is more than that of hydrated electron. The reason of the increase of $BP^{\bullet -}$ in THF observed here would be analogous to this previous report in water. At low BP concentration, most of the reaction 7 is not transferred to reaction 9 by reaction 5 because of the fast decay of reaction 7 and the low scavenging capacity. We speculate that the fast decay of reaction 7 is due to the e_{pre}^- which is distributed, in particular, near the parent radical cation. They recombine immediately with each other competing with solvation process, since the mobility of e_{pre}^- is much higher than that of e_{sol}^- and the short initial separation distance accelerates the geminate recombination. Upon addition of high concentration BP (e.g., >1 M), the e_{pre}^- which shows a fast geminate decay is partly scavenged by BP and the geminate ion recombination is decelerated due to the low mobility of $BP^{\bullet -}$. This delayed geminate ion recombination begins to appear at >1 M BP. The decays of $BP^{\bullet -}$ seems to converge on the flat level observed for relatively high concentration of BP (ca. 200 mM). This experimental fact supports the above speculation.

At extremely high concentration of BP (ca. >1 M), we should discuss the biphenyl radical cation ($BP^{\bullet +}$) formed by direct ionization of BP:

$$BP \rightsquigarrow BP^{\bullet +} + e_{pre}^- \qquad (15)$$

The contribution of $BP^{\bullet +}$ is statistically estimated according to the procedure in the previous report,[56] leading to roughly 30% $BP^{\bullet +}$ and 70% $THF^{\bullet +}$ just after the ionization in THF solution of 2 M BP. The positive charge of $BP^{\bullet +}$ is, however, immediately transferred to the surrounding THF, giving rise to BP and $THF^{\bullet +}$:

$$BP^{\bullet +} + THF \rightarrow BP + THF^{\bullet +} \qquad (16)$$

We measured the transient absorption spectra in THF solution of 2 M BP in the visible wavelength region from 600 to 750 nm. The $BP^{\bullet -}$ and $BP^{\bullet +}$ have the absorption peaks at 655 (extinction coefficient: $\epsilon = 12\ 500\ M^{-1}\ cm^{-1}$)[34,35,48,49] and 703 nm ($\epsilon = 14\ 500\ M^{-1}\ cm^{-1}$),[49,65] respectively. These extinction coefficients are almost equal; however, distinct absorption peak at 703 nm was not observed, supporting the immediate decay of $BP^{\bullet +}$ as expressed by reaction 16. This leads to the negligibly small concentration of $BP^{\bullet +}$, and thus, almost no contribution of $BP^{\bullet +}$ at around 400 nm, even though $BP^{\bullet +}$ itself has the strong absorption peaks at 365 and 367 nm.[49]

4. Summary

In order to conduct a comprehensive investigation on the reactivity of biphenyl with solvated electron and its precursor in THF, we carried out picosecond pulse radiolysis in the wavelength range from 400 to 900 nm and discrete 1300 nm. The initial decrease and subsequent scavenging reaction of solvated electrons were measured at 1300 nm where the absorption is mainly attributed to solvated electrons, and analyzed by considering overlap of solvated electrons and biphenyl radical anion, leading to $C_{37} = 87 \pm 3$ mM and $k_6 = 5.8 \pm 0.3 \times 10^{10}\ M^{-1}\ s^{-1}$. The kinetic traces at 408 nm, where the strongest peak of biphenyl radical anion lies, were analyzed according to the same procedure, demonstrating a consistency with the analysis at 1300 nm. The reaction radius between biphenyl and the solvated electron was found to be 0.44 nm from the rate constant obtained here and the diffusion constants of biphenyl and the solvated electron in the literature. At higher concentration of biphenyl (ca. >1 M), further increase of initial yield of biphenyl radical anion (ca. 10% at 2 M) was observed, accompanying a fast decay component. This fast decay, converging on the flat level found for the low concentration of biphenyl (ca. 200 mM), was explained by the scavenging reaction of precursor of solvated electron by biphenyl and subsequent delayed germinate ion recombination of biphenyl radical anion.

Acknowledgment. We would like to extend our gratitude to Dr. K. Okamoto at ISIR, Osaka University, for his help and encouragement. We would like to thank Prof. Y. Katsumura at the University of Tokyo for the discussion about C_{37}. We greatly appreciate the experimental support of Mr. S. Suemine and Mr. T. Yamamoto at ISIR, Osaka University. This work was supported in part by a grant-in-aid for scientific research from Ministry of Education, Culture, Sports, Science and Technology in Japan (MEXT).

References and Notes

(1) (a) Hart, E. J.; Anbar, M. *The Hydrated Electron*; John Wiley & Sons Inc.: New York, 1970. (b) In *Kinetics of Nonhomogenenous Processes*; Freeman, G. M. Ed.; John Wiley & Sons Inc.: New York, 1987. (c) In *Pulse Radiolysis*; Tabata, Y. Ed.; CRC press: Boca Raton, 1991. (d) In *Handbook of Radiation Chemistry*; Tabata, Y., Ito, Y., Tagawa, S. Eds.; CRC press: Boca Raton, 1991. (e) In *Radiation Chemistry: Present Status and Future Trends*; Jonah, C. D., Rao, B. S. M., Eds.; Studies in Physical and Theoretical Chemistry 87; Elsevier Science: New York, 2001. (f) In *Charged Particle and Photon Interactions with Matter*; Mozumder, A, Hatano, Y. Ed.; Marcel Dekker Inc.: New York, 2004.

(2) Hart, E. J.; Boag, J. W. *J. Am. Chem. Soc.* **1962**, *84*, 4090.

(3) (a) Wolff, R. K.; Bronskill, M. J.; Hunt, J. W. *J. Chem. Phys.* **1970**, *53*, 4211. (b) Aldrich, J. E.; Bronskill, M. J.; Wolff, R. K.; Hunt, J. W. *J. Chem. Phys.* **1971**, *55*, 530. (c) Wolff, R. K.; Aldrich, J. E.; Penner, T. L.; Hunt, J. W. *J. Phys. Chem.* **1975**, *79*, 210.

(4) Lam, K. Y.; Hunt, J. W. *Int. J. Radiat. Phys. Chem.* **1975**, *7*, 317.

(5) Hunt, J. W.; Chase, W. J. *Can. J. Chem.* **1977**, *55*, 2080.

(6) Jonah, C. D.; Miller, J. R.; Matheson, M. S. *J. Phys. Chem.* **1977**, *81*, 1618.

(7) (a) Lewis, M. A.; Jonah, C. D. *J. Phys. Chem.* **1986**, *90*, 5367. (b) Chernovitz, A. C.; Jonah, C. D. *J. Phys. Chem.* **1988**, *92*, 5946. (c) Jonah, C. D.; Bartels, D. M.; Chernovitz, A. C. *Radiat. Phys. Chem.* **1989**, *34*, 146.
(8) Hamill, W. H. *J. Phys. Chem.* **1969**, *73*, 1341.
(9) Peter, F. A.; Neta, P. *J. Phys. Chem.* **1972**, *76*, 630.
(10) Shiraishi, H.; Katsumura, Y.; Hiroishi, D.; Ishigure, K.; Washio, M. *J. Phys. Chem.* **1988**, *92*, 3011.
(11) Gauduel, Y.; Pommeret, S.; Yamada, N.; Migus, A.; Antonetti, A. *J. Am. Chem. Soc.* **1989**, *111*, 4974.
(12) Goulet, T.; Jay-Gerin, *Can. J. Chem.* **1992**, *96*, 5076.
(13) Keszei, E.; Murphrey, T. H. Rossky, P. J. *J. Phys. Chem.* **1995**, *99*, 22.
(14) Bartels, D. M.; Cook, A. R.; Mudaliar, M.; Jonah, C. D. *J. Phys. Chem. A* **2000**, *104*, 1686.
(15) Kambhampati, P.; Son, D. H.; Kee, T. W.; Barbara, P. F. *J. Phys. Chem. A* **2002**, *106*, 2374.
(16) (a) Jordan, K. D. *Science* **2004**, *306*, 618. (b) Bragg. A. E.; Verlet, J. R. R.; Kammrath, A.; Cheshnovsky, O.; Neumark, D. M. *Science* **2004**, *306*, 669. (c) Paik, D. H.; Lee, I. R.; Yang, D. S.; Baskin, J. S.; Zewail, A. H. *Science* **2004**, *306*, 672. (d) Hammer, N. I.; Shin, J. W.; Headrick, J. M.; Diken, E. G.; Roscioli, J. R.; Weddle, G. H.; Johnson, M. A. *Science* **2004**, *306*, 675.
(17) Muroya, Y.; Lin, M.; Wu, G.; Iijima, H.; Yoshii, K.; Ueda, T.; Kudo, H.; Katsumura, Y. *Radiat. Phys. Chem.* **2005**, *72*, 169.
(18) LaVerne, J. A.; Štefanič, I.; Pimblott, S. M. *J. Phys. Chem. A* **2005**, *109*, 9393.
(19) Lian, R.; Crowell, R. A.; Shkrob, I. A. *J. Phys. Chem. A* **2005**, *109*, 1510.
(20) Arai, S.; Sauer, M. C., Jr. *J. Chem. Phys.* **1966**, *44*, 2297.
(21) Bronskill, M. J.; Wolff, R. K.; Hunt, J. W. *J. Chem. Phys.* **1970**, *53*, 4201.
(22) Ražem, D.; Hamill, W. H. *J. Chem. Phys*. **1978**, *82*, 1460.
(23) Kenney-Wallace, G. A.; Jonah, C. D. *J. Phys. Chem.* **1982**, *86*, 2572.
(24) Pepin, C.; Goulet, T.; Houde, D.; Jay-Gerin, J.-P. *J. Phys. Chem.* **1994**, *98*, 7009.
(25) Dorfman, L. M.; Jou, F. Y.; Wageman, R. *Ber. Bunsenges. Phys. Chem*. **1971**, *75*, 681.
(26) (a) Brockrath, B.; Dorfman, L. M. *J. Phys. Chem.* **1973**, *77*, 1002. (b) Jou, F. Y.; Dorfman, L. M. *J. Chem. Phys.* **1973**, *58*, 4715. (c) Brockrath, B.; Gavlas, J. F.; Dorfman, L. M. *J. Phys. Chem.* **1975**, *79*, 3064.
(27) Baxendale, J. H.; Beaumond, D.; Rodgers, M. A. J. *Trans. Faraday Soc.* **1970**, *66*, 1996.
(28) Salmon, G. A.; Seddon, W. A.; Fletcher, J. W. *Can. J. Chem.* **1974**, *52*, 3259.
(29) Tran-Thi, T. H.; Koulkes-Pujo, A. M. *J. Phys. Chem.* **1983**, *87*, 1166.
(30) Kadhum, A. A. H.; Salmon, G. A. *J. Chem. Soc. Faraday Soc. 1* **1986**, *82*, 2521.
(31) Dalaire, J. A.; Delcourt, M. O.; Belloni, J. *J. Phys. Chem.* **1980**, *84*, 1186.
(32) Abramczyk, H.; Kroh, J. *Chem. Phys.* **1991**, *157*, 373.
(33) Martini, I. B.; Barthel, E. R.; Schwartz, B. J. *J. Chem. Phys.* **2000**, *113*, 11245.
(34) Renou, F.; Pernot, P.; Bonin, J.; Lampre, I.; Mostafavi, M. *J. Phys. Chem. A* **2003**, *107*, 6587.
(35) Renou, F.; Mostafavi, M.; Archirel, P.; Bonazzola, L.; Pernot, P. *J. Phys. Chem. A* **2003**, *107*, 1506.
(36) de Waele, V.; Sorgues, S.; Pernot, P.; Marignier, J. L. Monard, H.; Larbre, J. P.; Mostafavi, M. *Chem. Phys. Lett.* **2006**, *423*, 30.
(37) Nakano, A.; Kozawa, T.; Tagawa, S.; Szreder, T.; Wishart, J. F.; Kai, T.; Shimokawa, T. *Jpn. J. Appl. Phys.* **2006**, *45*, L197.
(38) Dye, J. L. *Acc. Chem. Res.* **1968**, *1*, 306.
(39) Delaire, J. A.; Bazouin, J. R. *Can. J. Chem*. **1979**, *57*, 2013.
(40) Wishart, J. F.; Neta, P. *J. Phys. Chem. B* **2003**, *107*, 7261.
(41) Grodkowski, J.; Neta, P.; Wishart, J. F. *J. Phys. Chem. A* **2003**, *107*, 9794.
(42) Smoluchowski, M. *Z. Phys. Chem.* **1917**, *92*, 129.
(43) Noyes, R. M. Proc. *React. Kinet.* **1961**, *1*, 129.
(44) Schwartz, H. A. *J. Chem. Phys.* **1971**, *55*, 3647.
(45) Czapski, G.; Peled, E. *J. Phys. Chem.* **1973**, *77*, 893.
(46) Miller, J. R.; *J. Chem. Phys.* **1972**, *56*, 5173.
(47) Miller, J. R.; Peeples, J. A.; Schmitt, M. J.; Closs, G. L. *J. Am. Chem. Soc.* **1982**, *104*, 6488.
(48) Jagur-Grodzinski, J.; Feld, M.; Yang, S. L.; Szwarc, M. *J. Phys. Chem.* **1965**, *69*, 628.
(49) Shida, T. *Electronic Absorption Spectra of Radical Ions*; Elsevier: Amsterdam, 1988.
(50) Saeki, A.; Kozawa, T.; Tagawa, S. *Nucl. Instr. Meth. A* **2006**, *556*, 391.
(51) Saeki, A.; Kozawa, T.; Okamoto, K.; Tagawa, S. *Jpn. J. Appl. Phys.*, in press.
(52) Saeki, A.; Kozawa, T.; Kashiwagi, S.; Okamoto, K.; Isoyama, G.; Yoshida, Y.; Tagawa, S. *Nucl. Instr. Meth. A.* **2005**, *546*, 627.
(53) Wollff, R. K.; M. J.; Bronskill, J. E.; Aldrich, J. W. Hunt. *J. Phys. Chem.* **1973**, *77*, 1350.
(54) Jonah, C. D. *Rev. Sci. Instrum.* **1975,** *46*, 62.
(55) In *Handbook of Chemistry and Physics*, 86th ed.; Lide, D. R. Ed.; CRC press: Boca Raton, FL, 2005.
(56) Saeki, A.; Kozawa, T.; Yoshida, Y.; Tagawa, S. *J. Phys. Chem. A* **2004**, *108*, 1475.
(57) (a) de Haas, M. P.; Warman, J. W.; Infelta, P. P.; Hummel, A. *Chem. Phys. Lett.* **1975**, *31*, 382. (b) Warman, J. W.; Infelta, P. P.; de Haas, M. P.; Hummel, A. *Chem. Phys. Lett.* **1976**, *43*, 321.
(58) (a) Sauer, M. C.; Trifunac, A. D.; McDonald, D. B.; Cooper, R. *J. Phys. Chem.* **1984**, *88*, 4096. (b) Trifunac, A. D.; Sauer, M. C.; Jonah, C. D. *Chem. Phys. Lett.* **1985**, *113*, 316. (c) Sauer, M. C.; Shkrob, I. A.; Yan, J.; Schmidt, K. H.; Trifunac, A. D. *J. Phys. Chem.* **1996**, *100*, 11325.
(59) (a) Shkrob, I. A.; Sauer, M. C.; Trifunac, A. D. *J. Phys. Chem.* **1996**, *100*, 7237. (b) Shkrob, I. A.; Liu, A. D.; Sauer, M. C.; Schmidt, K. H.; Trifunac, A. D. *J. Phys. Chem. B* **1998**, *102*, 3371.
(60) Kozawa, T.; Saeki, A.; Nakano, A.; Yoshida, Y.; Tagawa, S. *J. Vac. Sci. Tech. B* **2003**, *21*, 3149.
(61) Kozawa, T.; Saeki, A.; Yoshida, Y.; Tagawa, S. *Jpn. J. Appl. Phys.* **2002**, *41*, 4208.
(62) In *Handbook of Chemistry and Physics*, 86th ed.; Lide, D. R., Ed.; CRC press: Boca Raton, FL, 2005.
(63) Chang, P.; Slates, R. V.; Szwarc, M. *J. Phys. Chem.* **1966**, *70*, 3180.
(64) Heimlich, Y.; Rozenshtein, V.; Levanon, H.; Lukin, L. *J. Phys. Chem. A* **1999**, *103*, 2917.
(65) Gould, I. R.; Ege, D.; Moser, J. E.; Farid, S. *J. Am. Chem. Soc.* **1990**, *112*, 4290.